Proceedings of the Combustion Institute 41 (2025) 105978

Contents lists available at ScienceDirect

Proceedings of the Combustion Institute

journal homepage: www.elsevier.com/locate/proci

Generalized derivation of multi-step kinetic models for polymer condensed-phase pyrolysis: Application to poly(ethylene terephthalate)

Andrea Locaspi, Tiziano Faravelli *

Department of Chemistry, Materials, and Chemical Engineering "G. Natta", Politecnico di Milano, Milano, 20133, Italy

ARTICLE INFO

Keywords:
Poly(ethylene terephthalate)
Pyrolysis
Chemical reaction kinetics
Plastic waste
Condensed phase

ABSTRACT

From a circular economy perspective, plastic waste (PW) is a valuable source of chemicals, energy vectors and energy. This work presents a general methodology to derive multi-step kinetic models for the condensed-phase thermal decomposition of polymeric networks starting from fundamental physics-based models. This methodology, initially developed for vinyl polymers, is here extended and generalized to account for transient phenomena, interplay of molecular and radical pathways, and reaction systems where depolymerization does not play a major role. The approach is applied to PET as it is among the main components of PW, affects product quality, alters the release of chlorinated and nitrogenated compounds, and a validated physics-based semi-detailed mechanism (PET-85-700) is available. The lumping methodology allows to derive a multi-step model (PET-18-22) that employs 18 species and 22 condensed-phase reactions, achieving an 80 % reduction in species and 97 % decrease in reactions. This model is validated by comparison with PET-85-700 and literature experimental data on mass-loss profiles, volatile yields, and char characterization, demonstrating satisfactory agreement with the semi-detailed model predictions at a lower computational cost. The resulting CHEMKIN-like condensed-phase model is attached as Supplementary Materials and available online in the CRECK Modelling Lab GitHub repository. Extending the proposed approach to other polymers and coupling it with existing subsets in the CRECK kinetic framework (e.g., biomass, polyvinylchloride, polyethylene, polypropylene, polystyrene) offers a powerful tool to model thermochemical recycling of PW and biomass/PW mixtures.

1. Introduction

Large-scale industrial implementation of chemical recycling and waste valorization is critical for a sustainable chemical industry, supporting circular economy goals, and climate change mitigation [1,2]. Waste-to-Energy and Waste-to-Chemicals processes recover value also from complex feedstocks, such as plastic wastes (PW) and municipal solid wastes (MSW), via pyrolysis, combustion, or gasification [3]. Optimizing product distribution, designing experiments, reactors, and process and managing pollutant formation can greatly benefit from computational fluid dynamics (CFD) and chemical kinetic modelling, motivating this work.

Poly(ethylene terephthalate) (PET) is a major PW component due to its widespread use in packaging, fibers, films, and in the manufacturing and automotive industries [4]. Depending on region and season, PET content in PW samples ranges from 3 to 7 wt. % [5]. Despite its relatively low fraction, PET-derived oxygen significantly influences the entire product spectrum. It preferentially forms CO_2 and CO, leading to higher yields of low-value gas, and decreases the quality of pyrolysis oil due to the formation of benzoic acids and its derivatives [6]. Its aromatic rings also promote the formation of a carbonaceous solid residue (char), necessitating further downstream treatment. In addition, the presence of PET influences the release of chlorinated and nitrogenated compounds from polyvinylchloride (PVC) [7] and polyamides (PA) [7,8]. As formation of HCl and HCN are key challenges in PW thermochemical recycling and incineration, predicting PET degradation and its interactions with other polymers is essential.

While studies on PW combustion and gasification are emerging, condensed-phase degradation of pure polymers has been widely studied in the past decades [5]. This is because polymer pyrolysis is the first hierarchical step, while gasification/oxidation are secondary reactions that can be separately studied. PET thermal degradation has received less attention compared to other polymers [9]. Several reaction pathways have been investigated in scientific literature, but only global kinetic models have been proposed to the authors' knowledge. While suitable for large-scale simulations, these models lack predictive power

* Corresponding author.
E-mail address: tiziano.faravelli@polimi.it (T. Faravelli).

https://doi.org/10.1016/j.proci.2025.105978
Received 27 June 2025; Accepted 28 October 2025
Available online 8 November 2025

beyond tested conditions. Physics-based models, though computationally expensive, provide information also on condensed-phase changes and volatile release at different operating conditions [10], and can serve as foundation for simplified, yet physically representative kinetics [11]. Industrial applications require accurate but flexible models to predict residence times and product distribution, enabling use for reactor and process simulations. Multi-step models capture the phenomena involved while retaining the flexibility of global mechanism. These models can be employed to assess the effect of particle size, geometry, and transport phenomena, to design, model, and control industrial reactors.

This work proposes a generalized methodology for deriving CHEMKIN-like multi-step condensed-phase kinetic models from fundamental physics-based mechanisms. The methodology builds upon a previously developed approach for vinyl polymers [11], which simplifies the representation of polymeric chains, elementary radical chemistry, and product distribution into a limited number of global pyrolysis reactions. As this earlier approach is limited to polymers that mainly degrade via depolymerization, this work extends it to account for transient phenomena, molecular reactions, and mechanisms where unzipping is not a major pathway. This methodology is applied to PET thermal degradation, leveraging an existing semi-detailed kinetic model [10], but it can be readily extended to other polymeric networks when an elementary reaction-based model is available. The resulting kinetic model (PET-18-22) includes 18 species and 22 reactions and captures the degradation times and major products in a wide range of conditions, with similar accuracy to the starting model. The proposed methodology will be complemented by kinetic models for the secondary reactivity of volatiles and char, in line with previous works [12,13]. Coupling with other multi-step polymer [11] and biomass models [14] enables comprehensive and consistent description of PW and MSW thermochemical valorization. The model is attached as Supplementary Material (SM), it is openly available on GitHub [15], and can be directly employed for reactor and process simulations.

2. Condensed-phase kinetic mechanism

The present multi-step kinetic model describes the polymer degradation occurring in the condensed phase. The aim is to describe at low computational cost the thermochemical process in terms of evolution of the condensed-phase mass and formation of the major products. As the degradation mainly occurs above the polymer melting point [16], the initial material is assumed in the molten state. The pyrolysis process results in the formation of volatile compounds and a solid residue [10]. In the following, all compounds that evaporate from the molten to the gas phase are defined as "gas species". These are classified as light gases or tars according to their physical state at room temperature. Conversely, the solid residue is simply referred to as "char". The general pseudo-species, reaction classes and kinetic parameters are described in the following paragraphs.

2.1. Species definition

The plastic material is described through a single pseudo-species representative of the chemical moieties of the polymer. Considering PET, this species accounts for both the terephthalic and glycol units and is labelled *"P-PET-P"*. All polymeric chains longer than the trimer are represented with this functional group, while no molecular weight distinction is made in the present approach [11].

Low-molecular-weight (LMW) compounds are described similarly to conventional detailed models for gas and liquid-phase pyrolysis/oxidation [17]. To reduce the total number of species (N_s), only the main reaction products are introduced. Among light gases, the model considers CO, CO_2, CH_3CHO, and H_2. To account for variations in oxygen and hydrogen content, four monomer-like compounds are introduced: benzoic acid (BA) and vinyl benzoate (VB) are the main products of the radical mechanism, benzene (C_6H_6) represents all non-oxygenated products, and monovinyl terephthalate (MVT) lumps all mono-phthalate structures resulting from the molecular degradation (i.e., terephthalic acid, monovinyl terephthalate, and divinyl terephthalate). The dimers are represented by two species: *"DIMER"* represents dimers with carboxylic and vinyl ester terminations, while *"EGDB"* represents dimers with phenyl ends. Configurations with one phenyl and one acid or vinyl ester termination are represented as a mixture of these two species. In analogy with the other multi-step mechanisms [11], species with boiling temperature (T_b) <250 °C are assumed unreactive because of their fast boiling rates and form directly as gas-phase species, while only MVT, DIMER, and EGDB can undergo condensed-phase degradation before evaporating.

In line with the semi-detailed model [10], the solid residue is described with the fully lumped approach proposed for biomass pyrolysis [18]. Specifically, a single species labelled CHAR describes the aromatic structure, together with pseudo-species representative of oxygen and hydrogen moieties. The biomass model employs several species to describe chars' variation with thermal history, which however add limited information at increased computational cost. For this reason, the multi-step model considers only the high-temperature moieties G-COs, G-H_2, and CHARO. All solid-phase species are classified within the liquid subset, thereby avoiding a tri-phase system. This approach does not introduce any artificial dilution since the model considers only unimolecular reactions [10,11]. The model has N_s=18, with 1 species describing the polymeric material, 10 the gas-phase volatiles, 2 the liquid-phase volatiles, and 4 the solid residue. All liquid-phase species are identified by the *"(L)"* in their name.

2.2. Reaction mechanism

The condensed-phase degradation of PET occurs through a combination of molecular and radical pathways [9,10]. As mentioned, the multi-step model simplifies the complex reactivity into a few lumped single-step reactions (Fig. 1), each representative of multiple elementary acts. According to the semi-detailed model [10], PET decomposition begins via molecular reactions that promote radical formation. Unlike vinyl polymers, PET releases compounds smaller than the starting monomers, and does not undergo unzipping depolymerization due to the aromatic rings along the backbone. Consequently, the approach proposed for vinyl polymers [11] fails, as it relies on the unzipping of terminal radicals, thus motivating the present work. Although these are not explicitly considered in the multi-step model, their effects are incorporated through the rate parameters in order to capture the correct product selectivity [11].

The transient behavior of the semi-detailed model [10] is captured by introducing a correction to the rate parameters as modelling the time-dependent interplay of molecular and radical reactions requires introducing multiple species in antithesis to the aim of this work. The correction introduced consists in scaling down by a factor of 3 all rate parameters estimated a priori. The adjustment preserves the estimated selectivity, mildly affected by the unsteady radical concentration, while also correctly capturing the characteristic degradation times. This approach is applied only to the polymer species (P-PET-P), while it is not applied to the condensed-phase degradation of dimers. This distinction arises because low-molecular-weight products are released after the onset of radical degradation and are therefore mildly affected by the transient radical behavior. Employing the correct rate parameters also preserves the selectivity between degradation and evaporation predicted by the semi-detailed model. The introduced reaction classes and their rate parameters are summarized in Table 1 and discussed in detail in the next paragraphs.

The main degradation pathway is syn elimination, where the polymer decomposes to form carboxylic acid and vinyl esters. The introduced molecular reaction involves a single step that releases monomers and dimers with carboxylic and vinyl ester ends as:

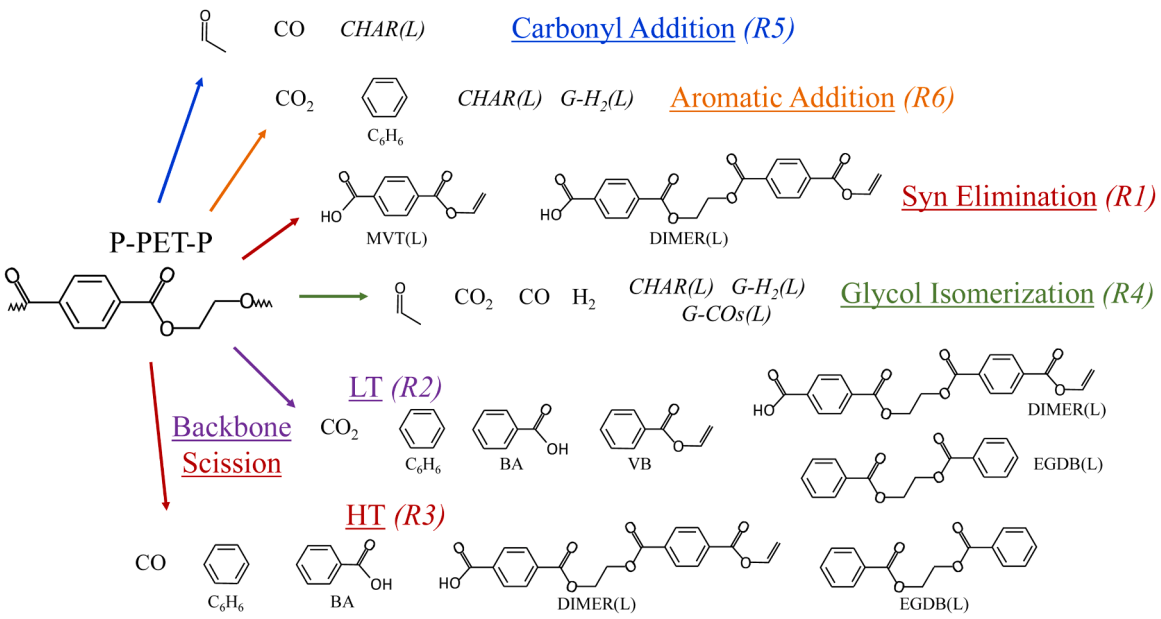

Fig. 1. Schematic representation of the multi-step degradation mechanism. Reactions are ordered by their temperature relevance: top low-T reactions, bottom high-T reactions.

Table 1
Reaction classes and their modified-Arrhenius parameters (units cm, mol, s, cal). $k = A \times \exp(-E_{act}/RT)$.

Reaction class (number)	A	E_{act}
(R1) Syn Elimination	1.0×10^{12}	48,000
(R2) Backbone scission LT	7.0×10^{14}	58,000
(R3) Backbone scission HT	2.8×10^{15}	62,000
(R4) Glycol isomerization	5.0×10^{12}	50,000
(R5) Carbonyl addition	1.5×10^{8}	37,000
(R6) Aromatic addition	$6.0 \times 10^{7} \times T$	45,000

$$\text{P-PET-P(L)} \rightarrow 1/3\text{MVT} + 1/3\text{DIMER(L)} \quad 2.0 \times 10^{12}\exp(-48000/RT) \tag{R1}$$

The reaction is first order in the concentration of the polymeric unit, and it releases equimolar amounts of monomer (MVT) and dimers. Other molecular reactions are neglected due to their lower importance. As the syn elimination rate does not depend on the location along the chain, (R1) employs the same elementary rate parameters of the semi-detailed model [10]. However, the frequency factor is 2/3 lower because of the global correction previously mentioned and as it lumps two reactive steps (monomer and dimer formation).

Estimating the importance of the radical degradation mechanism relies on the detailed knowledge of the radical families and their concentrations. In the case of PET, the main initiation sites are glycol units and, most importantly, the vinyl esters formed through the syn elimination [10]. For the lumping purpose, the radical families considered are phenylic ones ($\dot{P}h$) and alkyl-like ($\dot{A}$). The former are the main product of the decomposition reactions, while the latter are the most abundant family. Other radical families, e.g., carboxylic radicals, are neglected due to their fast decomposition or low relevance towards product selectivity. The choice of phenyl radicals is also motivated by their fast reactivity, which allows to estimate their concentration ($C_{\dot{P}h}$) through the pseudo-steady-state approximation on the semi-detailed mechanism (SD) [11]. The reactions leading to $\dot{P}h$ formation are β-scission of $\dot{A}$, while they are consumed by H-abstractions on any internal hydrogen (H_I) or by addition on aromatic rings in terephthalic units. The concentration of $\dot{A}$ is estimated as the difference between total radicals ($\dot{R}$) and phenylic ones. The total radical concentration ($C_{\dot{R}}$) is estimated through a pseudo-steady-state approximation as well [11], explicitly considering the impact of vinyl esters. The overall radical concentrations are therefore evaluated as:

$$C_{\dot{R}} = \sqrt{\left(k^{SD}_{RS} C_{PET} + k^{SD}_{RS,VE} C_{VE}\right) \Big/ k^{SD}_{RR}} \tag{1}$$

$$C_{\dot{P}h} \Big/ C_{\dot{R}} = \left(k^{SD}_{\beta LT} + k^{SD}_{\beta HT}\right) \Big/ \left(k^{SD}_{\beta,LT} + k^{SD}_{\beta,HT} + k^{SD}_{H_I,Ph} C_{H_I} + k^{SD}_{AA,Ph} C_{PET} + k^{SD}_{CA,Ph} C_{VE}\right) \tag{2}$$

$$C_{\dot{A}} = C_{\dot{R}} \left(1 - C_{\dot{P}h} / C_{\dot{R}}\right) \tag{3}$$

where C refers to concentrations, with C_{PET} being the concentration of backbone units ($C_{PET}=\rho_L/MW_{PET}$) C_{VE} the concentration of vinyl esters (VE), and C_{HI} the concentration of internal glycol hydrogen. The integral average amount of VE is computed from simulations of the semi-detailed model across a temperature range 300–900 °C [19], obtaining a value $C_{VE}=0.1C_{PET}$. k^{SD} are the rate constants of the semi-detailed model (Table S1 of the SM), with $k_{\beta,LT}$ and $k_{\beta,HT}$ being the β-scission constants respectively breaking the C(O)O—C bond or C(O)-OC bond, $k_{HI,Ph}$ the constant of H_I abstractions by phenyl radicals, and $k_{AA,Ph}$ and $k_{CA,Ph}$ the constant of aromatic and carbonyl addition by phenyl radicals.

The estimated radical concentrations are compared against the predictions of the semi-detailed model, verifying the correctness of the approach, and the global steps are then chosen based on the decomposition reactions of these radical families. In general, alkyl-like degradation pathways dominate at low temperatures, while phenyl radical additions become important at $T > 600$ °C. The main degradation pathway, responsible for formation of benzoic acid, CO_2 and CO, are alkyl-radical β-scissions. The multi-step model accounts for the same decomposition reactions of the semi-detailed mechanism, and therefore introduces two kinds of backbone degradation pathways as:

$$\text{P...PET...P(L)} \rightarrow 2/3\text{CO}_2 + 1/9\text{C}_6\text{H}_6 + 1/6\text{BA} + 1/6\text{VB} + 1/6\text{DIMER(L)} + 1/6\text{EGDB(L)} \quad 1.4 \times 10^{15}\exp(-58000/RT) \tag{R2}$$

$$\text{P...PET...P(L)} \rightarrow 4/3\text{CO} + 1/18\text{C}_6\text{H}_6 + 1/3\text{H}_2 + 1/3\text{BA} + 1/6\text{DIMER(L)} + 1/6\text{EGDB(L)} \quad 6.0 \times 10^{15}\exp(-62000/RT) \tag{R3}$$

These reactions lump the formation of monomers and dimers normalized on the number of chain-units consumed. These reactions represent the radical degradation mechanism being the main responsible for the formation of CO, CO_2, and phenyl ends, represented by BA, VB, and EGDB. The elementary rates of these reactions are estimated from the concentration of alkyl radicals and normalized on the mid-chain units. With respect to reaction (R2), the entrance channel is assumed to be rate-determining, and the multi-step rate is estimated as:

$$k_{(R2)} = k^{SD}_{\beta LT} C_{\dot{A}} \Big/ C_{PET} \tag{4}$$

and is regressed to an Arrhenius form. The rate of (R3) is estimated with the same approach, taking as reference the high-temperature beta-scission reaction of the semi-detailed model. The selectivity between (R2) and (R3) is the same as the semi-detailed model and controls the high-temperature CO/CO_2 ratio.

An additional pathway is introduced to account for alkyl radical isomerization to ethylidene structures, which leads to acetaldehyde formation from a 6-center elimination reaction [10]. The multi-step model introduces a single step that releases acetaldehyde while forming a phenyl anhydride:

$$\begin{aligned} &\text{P...PET...P(L)} \rightarrow \text{CH}_3\text{CHO} + \text{CO}_2 + 1/2\text{CO} + \text{H}_2 + 6\text{CHAR(L)} \\ &\quad + \text{G} - \text{H}_2\text{(L)} \; + 1/2\text{G} - \text{COs(L)} \\ &\quad 5.0 \times 10^{12} \exp(-50000/\text{RT}) \end{aligned} \tag{R4}$$

Because of its high thermal stability, the anhydride is represented with char's pseudo-species in analogy with the semi-detailed model [10]. To avoid introducing the species G-CO(L), G-COH_2(L) and their reactions, the multi-step model considers directly CO, G-COs(L) and G-H_2(L) as reaction products. The reaction rate is estimated as in Eq. (4), assuming isomerization being rate determining.

The multi-step model introduces two reactions representative of all radical addition pathways. The first pathway corresponds to additions to the carbonyl groups of vinyl esters releasing acetaldehyde and forming oxygenated char species and is written as:

$$\begin{aligned} &\text{P...PET...P(L)} \rightarrow 0.5\text{P...PET...P(L)} + \text{CH}_3\text{CHO} + 0.5\text{CO} \\ &\quad + 0.5\text{G} - \text{COs(L)} + 2\text{CHAR(L)} \\ &\quad 1.5 \times 10^{8} \exp(-37000/\text{RT}) \end{aligned} \tag{R5}$$

where the reaction products include 0.5P-PET-P as the resulting structure has half terephthalic and half glycol units. This reaction lumps both alkyl and phenyl radical additions, and the rate parameters of are estimated considering both pathways as:

$$k_{(R5)} = \left(k^{SD}_{CA,A} C_{\dot{A}} + k^{SD}_{CA,Ph} C_{\dot{Ph}} \right) C_{VE} \Big/ C_{PET} \tag{5}$$

where C_{VE}/C_{PET}=0.1 as previously estimated, and $k^{SD}_{CA,A}$ and $k^{SD}_{CA,Ph}$ are the carbonyl addition constant of alkylic and phenylic radicals of the semi-detailed model, respectively. This reaction is the main responsible for char formation at low temperatures. The second addition pathway introduced in the multi-step model represents additions to backbone aromatics forming CO_2 and oxygen-free char as:

$$\begin{aligned} &\text{P...PET...P(L)} \rightarrow 2\text{CO}_2 + 1/3\text{C}_6\text{H}_6 + 3\text{G} - \text{H}_2\text{(L)} + 6\text{CHAR(L)} \\ &\quad 6.0 \times 10^{7} \times \text{T} \times \exp(-45000/\text{RT}) \end{aligned} \tag{R6}$$

which lumps also the subsequent decarboxylations and β-scission of the radical product. Two CO_2 molecules are present as the reaction includes two decarboxylation steps, while $1/3C_6H_6$+H_2 substitutes ethylene to reduce N_s. The rate parameters are estimated as in Eq. (5), considering both VE and "*P-PET-P*" as addition sites. The rate constant is regressed to a modified-Arrhenius with a temperature exponent of 1 to capture in a single reaction the impact of both alkyl and phenylic radicals. Carbonyl additions do not require this, as alkyl radicals are more favored over phenylic ones for $T < 900$ °C. Conversely, phenyl radicals are favored in aromatic additions at $T > 700$ °C due to the higher energy barrier of alkyl radicals [10].

The same reaction classes are introduced also to model the condensed-phase degradation of MVT(L), DIMER(L) and EGDB(L). As mentioned, the rate parameters of these species do not consider the adjustment by 3 to properly represent the competition between evaporation and degradation. MVT can only undergo addition reactions, and a single step representing the sum of both reaction steps is introduced. To support broader use, pseudo-reactions are used to model evaporation, consistent with other polymer models [11]. The semi-detailed model [10] is also updated to employ evaporation reaction, and is also available on GitHub [15].

3. Results

The performances of the proposed lumping methodology are assessed by comparing the PET multi-step model with ~70 experimental datasets from the scientific literature and the starting semi-detailed model [10]. The validation targets are condensed-phase mass-loss profiles, volatile yields, and char characterization. Only experimental data on systems small enough to neglect transport limitations and secondary gas-phase reactions are considered. Since both chemistry and phase-changes are included in the kinetic mechanism, the equation for the mass of species j in phase P is:

$$dm^{P}_{j} \Big/ dt = R_{Lj} V_L MW_j \tag{6}$$

where R_{Lj} are molar formation/destruction rates of species j due to liquid-phase reactions, V_L the liquid-phase volume, and MWj the species molecular weight. Numerical integration is performed through the OpenSMOKE++ suite [20], employing a native fully-coupled solver for stiff systems. A broader validation is reported in the SM.

Fig. 2 shows the comparison of predicted and measured mass-loss profiles in dynamic (Fig. 2a) [21–24] and quasi-isothermal conditions (Fig. 2b) [23]. In general, the characteristic degradation times and temperatures are properly described in a broad range of heating rates (HR). Considering the significantly simplified kinetic mechanism, the model agrees with all experimental data within ~25 °C, and with the semi-detailed model within ~5 °C. Differences in model predictions stem both from the simplified reaction mechanism and char description. The former overestimates the onset reactivity, as it neglects the chain shortening, while the latter does not account for the low T physico-chemical evolution of char. For these 0D cases, simulation time is reduced by ~40–80 times compared to the semi-detailed mechanism on a common laptop, depending on operating conditions. Moreover, the reduced stiffness of the multi-step model can be further exploited in non-stiff solvers.

Fig. 3 shows a parity plot comparing multi-step (blue squares) and semi-detailed (orange circles) model predictions with experimental results [21–30] in dynamic conditions in terms of onset temperature ($T_{(mL=0.9)}$), 50 % degradation temperature ($T_{(mL=0.5)}$), and char yield. As mentioned, the multi-step model underestimates $T_{(mL=0.9)}$, as it neglects the chain shortening preceding volatile release, while capturing correctly $T_{(mL=0.5)}$. With respect to the char yield, the semi-detailed model already fails at capturing the high variability, reflected also in the multi-step model. The latter predicts a narrower distribution of char yields due to the more simplified description of char.

Fig. 4a shows the comparison of predicted and measured volatile mass yields. The multi-step model satisfactorily represents the prediction of the semi-detailed one, although with some specific deviation. The simplified description of monomers and dimers, represented only by MVT, EGDB and DIMER, does not properly account for their degradation to light gases. The multi-step model overestimates monomer formation as it neglects the condensed-phase degradation of MVT. The non-monotonic behavior predicted by the semi-detailed model results from the competition of decarboxylation reactions, which convert monomers

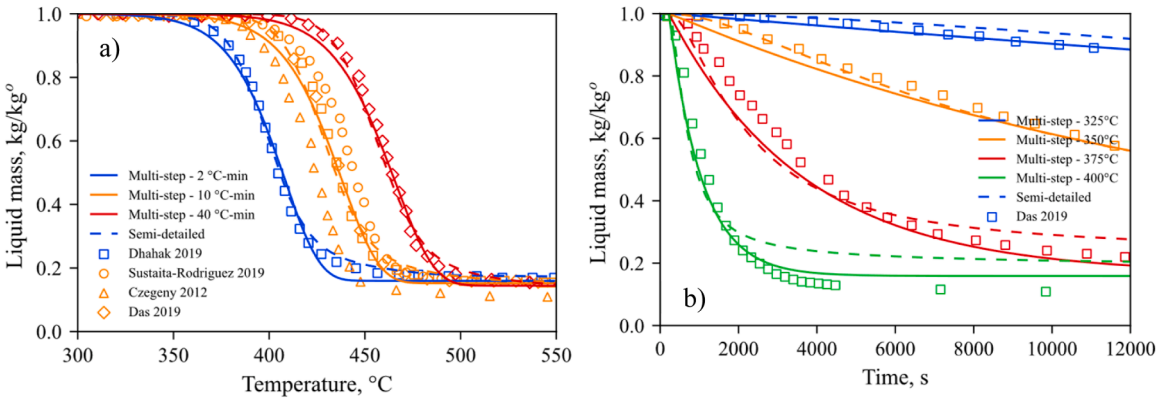

Fig. 2. PET mass-loss at: a) HR=2–40 °C/min; b) T = 325–400 °C. Comparison for multi-step (solid lines) and semi-detailed [10] (dashed lines) models with literature data (marks) [21–24].

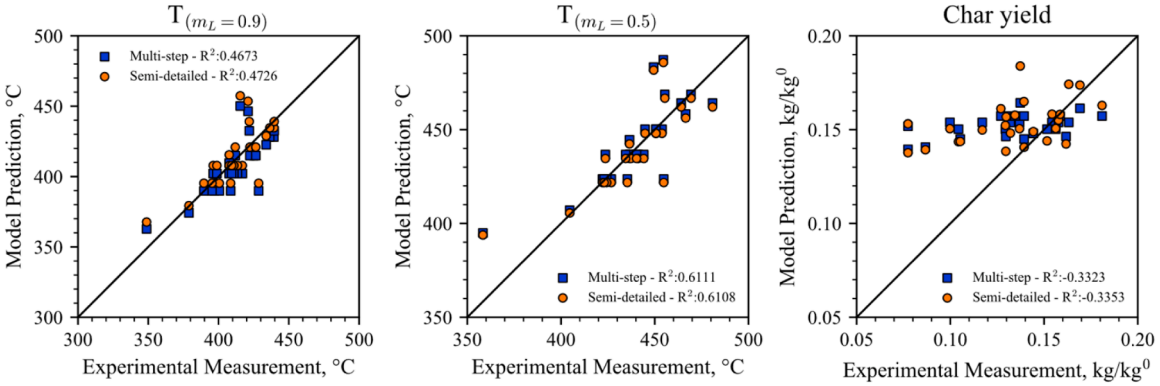

Fig. 3. Parity plots of model prediction with literature data [21–30] for PET degradation temperatures at sample mass (m_L) 0.9 and 0.5 and char yield.

to BA or VB, with the degradation of dimers, which forms monomers at high temperature. The overestimation of CO at low temperatures results from neglecting char deoxygenation and dumping it as light gases. The multi-step model overestimates the formation of mono-aromatic hydrocarbons (MAH) as the C_6H_6 species represents all non-oxygenated gases (e.g., light olefins). Fig. 4b shows the comparison between experimental measurements and model prediction with respect to the elemental composition of the residue. In general, increasing the temperature produces solid residues with high carbon content, while low temperature pyrolysis results in a higher oxygen content. The multi-step model captures this behavior, but predicts a mild influence of temperature because of the simplified description of char. For this reason, with respect to the semi-detailed model it predicts higher and lower carbon content at low and high temperatures, respectively. Nevertheless, the results of both models are satisfactory.

4. Conclusions

The present work proposes a generalized methodology to derive CHEMKIN-like multi-step condensed-phase kinetic models by guidance of physics-based kinetic models. The approach employs and improves lumping methodologies developed for vinyl polymers [11], which simplify the description of polymeric chains, radical chemistry, and product distribution in a few global degradation pathways. In the present work, the methodology is extended to account for transient phenomena, molecular reactions, and polymers where the reactivity of terminal radicals plays a minor role. Specifically, the methodology employs the physics-based model to investigate the main radical families and their elementary rates, by combining pseudo-steady-state assumptions for estimating radical concentrations, integral averages to recover transient phenomena, and rate-determining-step assumptions to lump complex reaction pathways. This approach also provides a quantitative evaluation of the relative importances of the reaction paths employed in the starting model.

The proposed methodology is applied to the thermal degradation of PET for validation purposes as an elementary reaction model is available [10]. The resulting kinetic model (PET-18–22), attached as SM, is validated with literature experimental data and the starting model in terms of mass-loss profiles, speciation, and char characterization. A reasonable accuracy is observed for the multi-step model, despite the 40–80 times decrease in computational cost, proving the reliability of the proposed lumping.

This methodology will be expanded to account for secondary cracking and oxidation reactions [12,13], while coupling it with other polymer [11] and biomass models [14] enables a comprehensive and consistent description of PW and MSW thermochemical valorization. All models are freely available on GitHub [15], and they can be employed to investigate the CFD of complex reactors and simulation of industrial process configurations.

Novelty and significance statement

This work presents a generalized methodology to bridge physics-based models, accurate but computationally expensive, and global models, flexible but case-specific. The methodology is employed to PET thermal degradation due to its relevance for plastic waste chemical recycling. A priori methods initially developed for polyolefin pyrolysis, are herein extended to capture competing molecular and radical reactivities, transient behaviors and multiple radical families with different reactivities. The resulting kinetic model is opensource and can

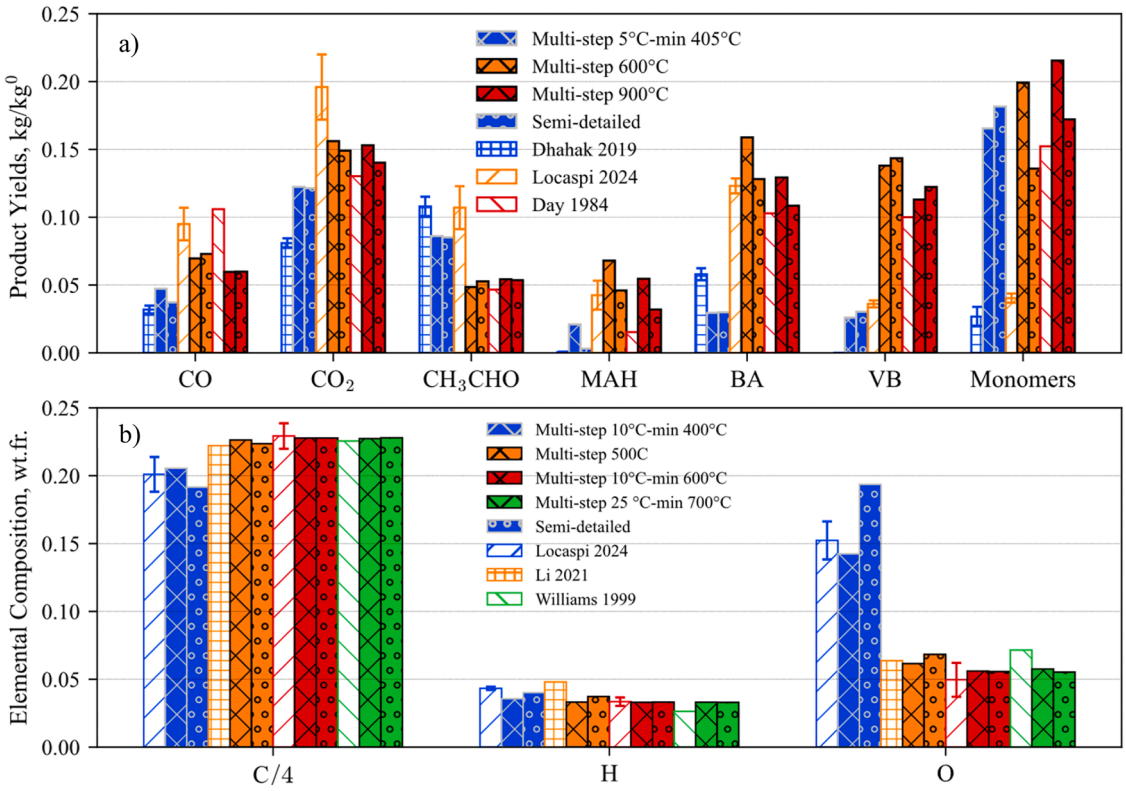

Fig. 4. Comparison of multi-step (solid circled bars) and semi-detailed [10] model (solid dashed bars) with experimental data (empty bars) for PET: a) final species mass yields [10,21,31]; b) char elemental analysis [10,32,33].

be coupled with other multi-step mechanisms for polymers and biomass. The model is validated against both the starting model and available literature data on mass loss, volatile distribution, and char characterization, achieving a 40–80 times decrease in computational cost on common laptops. The model is fully predictive, requiring no case-specific tuning, and will be extended to target all plastic waste components.

Disclaimer

This project was funded by the United States Department of Energy, National Energy Technology Laboratory, in part, through a site support contract. Neither the United States Government nor any agency thereof, nor any of their employees, nor the support contractor, nor any of their employees, makes any warranty, express or implied, or assumes any legal liability or responsibility for the accuracy, completeness, or usefulness of any information, apparatus, product, or process disclosed, or represents that its use would not infringe privately owned rights. Reference herein to any specific commercial product, process, or service by trade name, trademark, manufacturer, or otherwise does not necessarily constitute or imply its endorsement, recommendation, or favoring by the United States Government or any agency thereof. The views and opinions of authors expressed herein do not necessarily state or reflect those of the United States Government or any agency thereof.

CRediT authorship contribution statement

Andrea Locaspi: Writing – original draft, Visualization, Validation, Methodology, Investigation, Conceptualization. **Tiziano Faravelli:** Writing – review & editing, Supervision, Project administration, Funding acquisition.

Declaration of competing interest

The authors declare that they have no known competing financial interests or personal relationships that could have appeared to influence the work reported in this paper.

Acknowledgements

This work was performed in support of the U.S. Department of Energy's (DOE) Office of Fossil Energy and Carbon Management's Gasification Program and executed through the National Energy Technology Laboratory (NETL) Research & Innovation Center's Advanced Reaction Systems Field Work Proposal. This project has received funding from the European Union's Horizon Europe research and innovation programme under the HORIZON—CL4–2021-TWIN-TRANSITION-01 grant agreement No 101058412. Views and opinions expressed are however those of the author(s) only and do not necessarily reflect those of the European Union or HADEA. Neither the European Union nor the granting authority can be held responsible for them.

Supplementary materials

Supplementary material associated with this article can be found, in the online version, at doi:10.1016/j.proci.2025.105978.

References

[1] A.R. Rahimi, J.M. Garciá, Chemical recycling of waste plastics for new materials production, Nat. Rev. Chem. 16 (1) (2017) 1–11, 2017.
[2] K.M. Van Geem, Plastic waste recycling is gaining momentum, Science 381 (2023) 607–608 (80-.).
[3] U. Arena, Process and technological aspects of municipal solid waste gasification. A review, Waste Manag. 32 (2012) 625–639.
[4] K. Ragaert, L. Delva, K. Van Geem, Mechanical and chemical recycling of solid plastic waste, Waste Manag. 69 (2017) 24–58.

[5] O. Dogu, M. Pelucchi, R. Van de Vijver, P.H.M. Van Steenberge, D.R. D'hooge, A. Cuoci, M. Mehl, A. Frassoldati, T. Faravelli, K.M. Van Geem, The chemistry of chemical recycling of solid plastic waste via pyrolysis and gasification: state-of-the-art, challenges, and future directions, Prog. Energy Combust. Sci. 84 (2021) 100901.
[6] M.S. Talmadge, R.M. Baldwin, M.J. Biddy, R.L. McCormick, G.T. Beckham, G. A. Ferguson, S. Czernik, K.A. Magrini-Bair, T.D. Foust, P.D. Metelski, C. Hetrick, M. R. Nimlos, A perspective on oxygenated species in the refinery integration of pyrolysis oil, Green Chem. 16 (2014) 407–453.
[7] I. Coralli, V. Giorgi, I. Vassura, A.G. Rombolà, D. Fabbri, Secondary reactions in the analysis of microplastics by analytical pyrolysis, J. Anal. Appl. Pyrolysis 161 (2022) 105377.
[8] R. Knümann, H. Bockhorn, Investigation of the kinetics of pyrolysis of PVC by TG-MS-analysis, Combust. Sci. Technol. 101 (1994) 285–299.
[9] A. Locaspi, M. Ferri, F. Serse, M. Maestri, M. Pelucchi, Chemical Kinetics of Catalytic/Non-Catalytic Pyrolysis and Gasification of Solid Plastic Wastes, Academic Press, 2022.
[10] A. Locaspi, O. Akin, D. Withoeck, M. Havaei, A. Frassoldati, L.P. Maffei, M. Pelucchi, M. Mehl, R.J. Varghese, K.M. Van Geem, T. Faravelli, A lumped kinetic model and experimental investigation of poly(ethylene terephthalate) condensed-phase pyrolysis, Chem. Eng. J. 500 (2024) 156955.
[11] A. Locaspi, A. Frassoldati, T. Faravelli, Reduced-order condensed-phase kinetic models for polyethylene, polypropylene and polystyrene thermochemical recycling, Chem. Eng. J. (2024) 156949.
[12] A. Locaspi, A. Pergurri, M. Mehl, M. Pelucchi, S. Natesakhawat, H. Zhou, Y. Xu, P. Wang, M. Shahnam, T. Faravelli, A semi-detailed pyrolytic gas-phase kinetic model for the volatiles of polyethylene thermal degradation, Proc. Combust. Inst. 41 (2025) 105912.
[13] A. Locaspi, P. Debiagi, M. Pelucchi, C. Hasse, T. Faravelli, A predictive physico-chemical model of biochar oxidation, Energy and Fuels 35 (2021) 14894–14912.
[14] E. Ranzi, P.E.A. Debiagi, A. Frassoldati, Mathematical modeling of fast biomass pyrolysis and bio-oil formation. Note I: kinetic mechanism of biomass pyrolysis, ACS Sustain. Chem. Eng. 5 (2017) 2867–2881.
[15] CRECK Modeling Lab, Kinetic-mechanisms. https://github.com/CRECKMODELING/Kinetic-Mechanisms, 2025.
[16] G.W. Halek, Zero-order kinetics of acetaldehyde thermal generation from polyethylene terephthalate, J. Polym. Sci. Part C, Polym. Symp. (1986) 83–92.
[17] M. Dente, G. Bozzano, T. Faravelli, A. Marongiu, S. Pierucci, E. Ranzi, Kinetic modelling of pyrolysis processes in gas and condensed phase, Adv. Chem. Eng. 32 (2007) 51–166.
[18] X. Zou, P. Debiagi, M.A. Amjed, M. Zhai, T. Faravelli, Impact of high-temperature biomass pyrolysis on biochar formation and composition, J. Anal. Appl. Pyrolysis 179 (2024) 106463.
[19] A. Pegurri, T. Dinelli, L. Pratali Maffei, T. Faravelli, A. Stagni, Coupling chemical lumping to data-driven optimization for the kinetic modeling of dimethoxymethane (DMM) combustion, Combust. Flame 260 (2024) 113202.
[20] A. Cuoci, A. Frassoldati, T. Faravelli, E. Ranzi, Numerical modeling of auto-ignition of isolated fuel droplets in microgravity, Proc. Combust. Inst. 35 (2015) 1621–1627.
[21] A. Dhahak, G. Hild, M. Rouaud, G. Mauviel, V. Burkle-Vitzthum, Slow pyrolysis of polyethylene terephthalate: online monitoring of gas production and quantitative analysis of waxy products, J. Anal. Appl. Pyrolysis 142 (2019) 104664.
[22] Z. Czégény, E. Jakab, M. Blazsó, T. Bhaskar, Y. Sakata, Thermal decomposition of polymer mixtures of PVC, PET and ABS containing brominated flame retardant: formation of chlorinated and brominated organic compounds, J. Anal. Appl. Pyrolysis 96 (2012) 69–77.
[23] P. Das, P. Tiwari, Thermal degradation study of waste polyethylene terephthalate (PET) under inert and oxidative environments, Thermochim. Acta 679 (2019) 178340.
[24] J.M. Sustaita-Rodríguez, F.J. Medellín-Rodríguez, D.C. Olvera-Mendez, A. J. Gimenez, G. Luna-Barcenas, Thermal stability and early degradation mechanisms of high-density polyethylene, polyamide 6 (Nylon 6), and polyethylene terephthalate, Polym. Eng. Sci. 59 (2019) 2016–2023.
[25] A. Dhahak, C. Grimmer, A. Neumann, C. Rüger, M. Sklorz, T. Streibel, R. Zimmermann, G. Mauviel, V. Burkle-Vitzthum, Real time monitoring of slow pyrolysis of polyethylene terephthalate (PET) by different mass spectrometric techniques, Waste Manag. 106 (2020) 226–239.
[26] I. Martín-Gullón, M. Esperanza, R. Font, Kinetic model for the pyrolysis and combustion of poly-(ethylene terephthalate) (PET), J. Anal. Appl. Pyrolysis 58–59 (2001) 635–650.
[27] M. Brebu, T. Bhaskar, K. Murai, A. Muto, Y. Sakata, M.A. Uddin, The effect of PVC and/or PET on thermal degradation of polymer mixtures containing brominated ABS, Fuel 83 (2004) 2021–2028.
[28] J. Moltó, R. Font, J.A. Conesa, Kinetic model of the decomposition of a PET fibre cloth in an inert and air environment, J. Anal. Appl. Pyrolysis. 79 (2007) 289–296.
[29] A. Brems, J. Baeyens, J. Beerlandt, R. Dewil, Thermogravimetric pyrolysis of waste polyethylene-terephthalate and polystyrene: a critical assessment of kinetics modelling, Resour. Conserv. Recycl. 55 (2011) 772–781.
[30] S.R. Horton, J. Woeckener, R. Mohr, Y. Zhang, F. Petrocelli, M.T. Klein, Molecular-level kinetic modeling of the gasification of common plastics, Energy & Fuels 30 (2016) 1662–1674.
[31] M. Day, D.M. Wiles, Influence of temperature and environment on the thermal decomposition of poly(ethylene terephthalate) fibres with and without the flame retardant tris(2,3-dibromopropyl) phosphate, J. Anal. Appl. Pyrolysis 7 (1984) 65–82.
[32] C. Li, F. Ataei, F. Atashi, X. Hu, M. Gholizadeh, Catalytic pyrolysis of polyethylene terephthalate over zeolite catalyst: characteristics of coke and the products, Int. J. Energy Res. 45 (2021) 19028–19042.
[33] E.A. Williams, P.T. Williams, The pyrolysis of individual plastics and a plastic mixture in a fixed bed reactor, J. Chem. Technol. Biotechnol. 70 (1997) 9–20.